


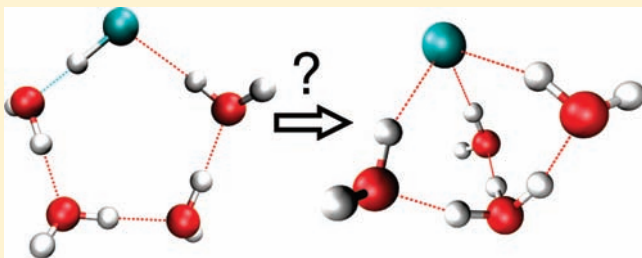
Aggregation-Induced Chemical Reactions: Acid Dissociation in Growing Water Clusters

Harald Forbert,^{*} Marco Masia,[†] Anna Kaczmarek-Kedziera,[‡] Nisanth N. Nair,[§] and Dominik Marx

Lehrstuhl für Theoretische Chemie, Ruhr-Universität Bochum, 44780 Bochum, Germany

 Supporting Information

ABSTRACT: Understanding chemical reactivity at ultracold conditions, thus enabling molecular syntheses via interstellar and atmospheric processes, is a key issue in cryochemistry. In particular, acid dissociation and proton transfer reactions are ubiquitous in aqueous microsolvation environments. Here, the full dissociation of a HCl molecule upon stepwise solvation by a small number of water molecules at low temperatures, as relevant to helium nanodroplet isolation (HENDI) spectroscopy, is analyzed in mechanistic detail. It is found that upon successive aggregation of HCl with H₂O molecules, a series of cyclic heteromolecular structures, up to and including HCl(H₂O)₃, are initially obtained before a precursor state for dissociation, HCl(H₂O)₃ ··· H₂O, is observed upon addition of a fourth water molecule. The latter partially aggregated structure can be viewed as an “activated species”, which readily leads to dissociation of HCl and to the formation of a solvent-shared ion pair, H₃O⁺(H₂O)₃Cl⁻. Overall, the process is mostly downhill in potential energy, and, in addition, small remaining barriers are overcome by using kinetic energy released as a result of forming hydrogen bonds due to aggregation. The associated barrier is not ruled by thermal equilibrium but is generated by athermal non-equilibrium dynamics. These “aggregation-induced chemical reactions” are expected to be of broad relevance to chemistry at ultralow temperature much beyond HENDI spectroscopy.



1. INTRODUCTION

The dissociation of Brønsted acids, proton transfer, and ion solvation in bulk water is a core subject in physical chemistry and chemical physics.^{1–4} Much insight has been extracted at the molecular level using experiment^{1,2,5–8} as well as computer simulation^{3,4,9–17} (to cite but a few). In stark contrast, the dissociation of acids in confined geometries as provided by surfaces, interfaces, or small clusters is an issue of much current research. In the realm of microsolvation, a plethora of theoretical studies focused on dissociation of archetypal acids such as HCl, HBr, and others in typically small water clusters consisting of a fixed number of molecules,^{18–44} whereas the experimental literature on this subject is rather scarce.^{45–54} Prime issues of the computational studies typically revolve around the determination of stable molecular versus dissociated structures given a certain number of water molecules, the related aspect of how many water molecules are necessary to allow for stable dissociation, and finally the dissociation mechanism itself as a function of a fixed number of water molecules.

In the case of HCl(H₂O)_{*n*} clusters, theoretical studies such as refs 20,23,29,35,42 support the idea that four H₂O molecules might provide the smallest possible hydrogen-bonded water network, which can host a fully dissociated HCl molecule as a charge-separated solvent-shared ion pair, H₃O⁺(H₂O)₃Cl⁻, labeled “SIP” in Figure 1. The zwitterionic SIP is the most compact hydrogen-bonded network wherein a hydronium core, H₃O⁺, forms an Eigen complex,⁴ that is, H₃O⁺(H₂O)₃, by

donating three hydrogen bonds to the three remaining water molecules, which in turn can microsolvate Cl⁻ by creating an anionic solvation shell. The most favored undissociated (UD), molecular HCl(H₂O)₄ species is also a minimum on the *n* = 4 potential energy surface (PES); this is best characterized as a flat, five-membered ring where HCl replaces a water molecule by acting as a hydrogen-bond donor and acceptor; see Figure 1. UD features a ring-like, hydrogen-bonding topology, where HCl is incorporated like a single-donor, single-acceptor water molecule, whereas the SIP dissociation product is most compact, with three water molecules sandwiched between a hydronium cation and the Cl⁻ anion. Therefore, the barriers for interconversion are expected to be very high. Thus, computational investigations that attempted to elucidate the dissociation mechanism traditionally concentrated on locating low-barrier pathways that allow for the drastic topology changes that connect UD with SIP, possibly involving low-lying intermediates, such as, for example, the contact ion pair (CIP); see Figure 1.

On the basis of this line of thinking, the traditional paradigm for finding out the smallest number of water molecules needed to support acid dissociation in finite water clusters such as HCl(H₂O)_{*n*} adheres to the following computational protocol: First, various undissociated and dissociated (local) minima are located on the PES for a given number of solvent molecules around a

Received: November 16, 2010

Published: February 25, 2011

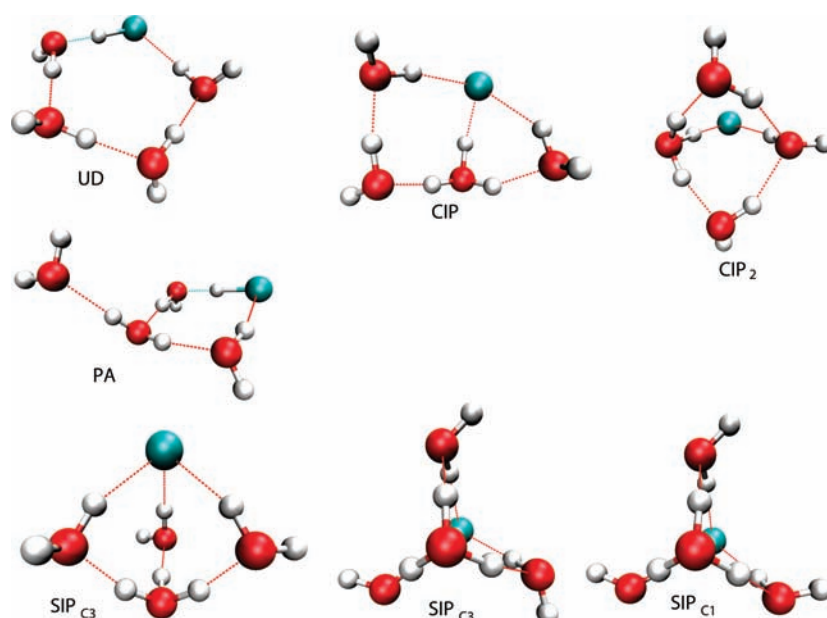


Figure 1. Optimized structures of the discussed $\text{HCl}(\text{H}_2\text{O})_4$ species: undissociated (UD), contact ion pair (CIP), compact contact ion pair (CIP_2), partially aggregated (PA), solvent-shared ion pair (SIP) with C_3 and C_1 conformation, SIP_{C_3} , and SIP_{C_1} , respectively, as determined by the orientation of the water molecule in the lower right corner (of the structures in the center and to the right in the bottom row). The SIP_{C_3} structure is shown in two orientations to reveal better the hydrogen-bond topology. Note that all structural parameters such as bond lengths, which are not needed for the purpose of this study, can be extracted from the data compiled in the Supporting Information.

solute molecule using structure optimization, possibly following extensive annealing procedures. Second, the most stable undissociated and dissociated structures are determined for a given number of solvent molecules. Third, the minimum number of solvent molecules where the most stable dissociated structure is lower in energy as compared to the most stable undissociated structure is determined. Fourth, minimum energy pathways that connect these two structures are mapped out, and the transition states are computed using the minimum number of solvent molecules. Fifth, the pathway that features the lowest energy barrier overall is said to govern dissociation at the determined cluster size. Thus, the standard approach to understand acid dissociation in finite clusters is to first build a cluster using all molecules involved and, only subsequently, find out how dissociation can take place for the given number of solvent molecules.

In a recent joint experimental and simulation effort, a distinctly different scenario for acid dissociation in small water clusters has been revealed⁵⁵ (see also ref 56). Using the pickup technique,⁵⁷ these experiments⁵⁵ were carried out in superfluid ^4He -nanodroplets, which are known to be able to efficiently cool molecules to temperatures of less than 1 K.^{57–59} Using high-resolution, mass-selective infrared laser spectroscopy, evidence has been provided that microsolvated hydronium H_3O^+ , that is, the elementary dissociation product of HCl in water,⁴ can be formed when one HCl molecule interacts with exactly four H_2O molecules. However, given that 1 K corresponds to thermal energies of roughly 0.01 kJ/mol per degree of freedom, the disturbing question arises of how the above-mentioned, 1000-fold higher dissociation barriers (of the order of 10 kJ/mol) can be surmounted at all in such ultracold environments. The puzzle has been solved via the use of ab initio molecular dynamics simulations,⁶⁰ which demonstrate that undissociated clusters assemble by stepwise water molecule addition up to adding three

H_2O to one HCl, thus yielding a hydrogen-bonded, ring-like $\text{HCl}(\text{H}_2\text{O})_3$ structure. Adding a fourth water molecule to this undissociated $n = 3$ species then spontaneously yields the dissociated SIP, $\text{H}_3\text{O}^+(\text{H}_2\text{O})_3\text{Cl}^-$. Note that this species is sometimes termed a solvent-separated ion pair in the cluster or microsolvation literature, whereas the term solvent-shared ion pair is used when discussing bulk solvation phenomena (see, for instance, p 53 in ref 61). This so-called “aggregation-induced dissociation” mechanism⁵⁵ bypasses deep local energy minima on the $n = 4$ PES, such as the UD structure, and thus avoids having to surmount high-lying transition states toward the SIP product. Another key aspect of this class of mechanisms is to convert potential energy gained upon aggregation, that is, the binding energy due to the formation of hydrogen bonds as a result of adduct formation, into kinetic energy, thus inducing athermal fluctuations, which allow the remaining (sufficiently low) barriers to be overcome; see Figure 2 for illustration.

Greatly transcending our preliminary report,⁵⁵ in this Article we investigate in great detail at the molecular level the two very different mechanisms that lead to HCl dissociation, both involving exactly four microsolvating water molecules. The traditional mechanism is presented by locating minima, transition states, and the connecting rearrangement pathway on the free energy surface (FES) in a subspace spanned by two appropriate reaction coordinates. This mechanism starts from the undissociated $\text{HCl}(\text{H}_2\text{O})_4$ reactant structure (UD), proceeds via a partially dissociated contact ion pair (CIP) intermediate, and ends in the fully dissociated solvent-shared ion pair (SIP) product, $\text{H}_3\text{O}^+(\text{H}_2\text{O})_3\text{Cl}^-$, which is the global minimum on this FES; see Figure 1 for these structures. Second, a set of so-called aggregation simulations is used to study the novel reaction mechanism that allows for dissociation into SIP without initially performing the molecular UD structure. An important ingredient, as opposed to the CIP intermediate in the traditional mechanism, is a

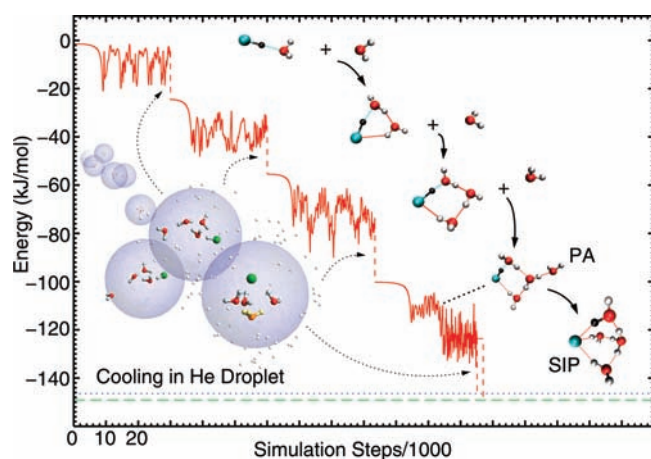


Figure 2. Simulation of a stepwise aggregation process leading to aggregation-induced dissociation of $\text{HCl}(\text{H}_2\text{O})_n$ from $n = 3$ to $n = 4$ according to the sequence $\text{HCl} + 4\text{H}_2\text{O} \rightarrow \text{HCl}(\text{H}_2\text{O}) + 3\text{H}_2\text{O} \rightarrow \text{HCl}(\text{H}_2\text{O})_2 + 2\text{H}_2\text{O} \rightarrow \text{HCl}(\text{H}_2\text{O})_3 + \text{H}_2\text{O} \rightarrow \text{H}_3\text{O}^+(\text{H}_2\text{O})_3\text{Cl}^-$. The optimized structures for the $n = 4$ partially aggregated (PA) and solvent-shared ion pair species (SIP) are explicitly labeled. The proton derived from HCl is marked in black in all structures. The solid red lines show the evolution of the potential energy on the scale given by the binding energy (i.e., $E[\text{HCl}(\text{H}_2\text{O})_n] - E[\text{HCl}] - nE[\text{H}_2\text{O}]$) obtained from representative aggregation simulations as a function of the ab initio molecular dynamics step. Vertical dashed red lines symbolize cooling of the aggregation product (obtained via full structure optimization) inside the helium droplet (schematically represented in the inset) before the next aggregation simulation commences. Horizontal dashed green and dotted blue lines mark the binding energies of $\text{SIP}_{\text{C}3}$ and $\text{SIP}_{\text{C}1}$, respectively. Reprinted with permission from ref 55. Copyright 2009 Science Magazine, AAAS.

partially aggregated (PA) undissociated structure, $\text{HCl}(\text{H}_2\text{O})_3 \cdots \text{H}_2\text{O}$, where a water molecule accepts a hydrogen bond from the cyclic four-membered $\text{HCl}(\text{H}_2\text{O})_3$ ring; see Figure 1. The PA arrangement can be viewed as an “activated” precursor species that leads preferentially and directly to the fully dissociated SIP product. Characterizing this peculiar aggregation-induced dissociation mechanism⁵⁵ and contrasting it with respect to the traditional mechanism is the main focus of this Article.

2. METHODS

All calculations have been carried out in the framework of density functional theory using the BLYP functional,^{62,63} a plane wave basis set with a cutoff of 70 Ry, and norm-conserving pseudopotentials.⁶⁴ A cubic supercell of length 20.0 Å was used, and cluster boundary conditions were applied to properly treat isolated systems.⁶⁰ All calculations reported here have been carried out using the CPMD simulation package.^{60,65} It should be noted that the accuracy of this electronic structure approach in describing the structure and dynamics of $\text{HCl}(\text{H}_2\text{O})_n$ clusters has been previously assessed thoroughly for $n = 0$ up to $n = 6$, including various molecular and dissociated species where appropriate.⁴²

2.1. Free Energy Simulations. Metadynamics⁶⁶ is a useful technique for computing multidimensional free energy surfaces (FES) at a predefined temperature in a subspace spanned by a suitable set of generalized coordinates using coarse-grained, non-Markovian dynamics. The method, developed by Laio and Parrinello,⁶⁶ is based on the gradual buildup of a history-dependent biasing potential that discourages the

system from revisiting points in configurational space. In this way, the added biasing potential pushes the system far from the reactant minima of the FES, thus allowing the sampling of important but unfavorable intermediate and transition states. The FES is readily obtained from the accumulated biasing potential. Here, the extended Lagrangian formulation⁶⁷ in conjunction with the efficient Car–Parrinello approach⁶⁸ to ab initio molecular dynamics is used. A detailed discussion of the method can be found in refs 60,69,70.

The generalized coordinates themselves, which are called collective variables (CVs), can depend on many Cartesian or internal degrees of freedom and thus allow for a great flexibility. To study HCl dissociation in a finite water cluster, two CVs were devised to drive, and eventually observe the reaction of, the $\text{HCl}(\text{H}_2\text{O})_4$ system from the undissociated (UD) molecular initial state to the most stable global minimum, that is, the dissociated solvent-shared ion pair (SIP). Building upon insights gained from previous canonical ab initio simulations⁴² of UD, contact ion pair (CIP), and SIP structures, the CVs were constructed such that they take into account both changes of chlorine solvation by water molecules and structural reorganization of water molecules as represented by the respective oxygens. The first CV is defined to be the coordination number $\text{CN}_{\text{Cl}-\text{O}}$ of chlorine with respect to all oxygens:

$$\text{CN}_{\text{Cl}-\text{O}} = \sum_{j=1}^{n_{\text{O}}} \left[\frac{1 - \left(\frac{r_{\text{Cl}-\text{O}_j}}{r_0} \right)^m}{1 - \left(\frac{r_{\text{Cl}-\text{O}_j}}{r_0} \right)^n} \right] \quad (1)$$

where the cutoff distance r_0 was set to 3.7 Å and $m = 6$ and $n = 12$. Furthermore, a repulsive potential was located at $\text{CN}_{\text{Cl}-\text{O}} = 1.5$ to prevent HCl to detach in molecular form from the water cluster. With this choice of parameters, $\text{CN}_{\text{Cl}-\text{O}}$ is ~ 2 for UD and PA, ~ 2.5 for CIP, and ~ 3 for SIP. The second CV is defined to be the dihedral angle ϕ formed by the four oxygen atoms. Its value varies from $\sim 160^\circ$ for UD via $\sim 100^\circ$ for CIP to $\sim 50^\circ$ for both SIP and PA. Taken together, $\text{CN}_{\text{Cl}-\text{O}}$ and ϕ allow one to distinguish all species relevant to investigate dissociation of $\text{HCl}(\text{H}_2\text{O})_4$.

The width and height of the spherical Gaussians^{60,69,70} underlying the non-Markovian sampling of minima according to metadynamics were set to $W = 0.04$ and $H = 0.0004 \text{ au} \approx 2k_{\text{B}}T \approx 1 \text{ kJ/mol}$, respectively. The temperature of the CVs was controlled via velocity rescaling, whereas the temperature of the nuclei was thermostatted using Nosé–Hoover chains⁶⁰ at 50 K to establish the canonical ensemble, thus yielding Helmholtz free energies; the orbital degrees of freedom were also coupled to Nosé–Hoover chains to ensure Car–Parrinello adiabaticity.⁶⁰ A time step of 0.121 fs was used together with a fictitious mass parameter for the orbitals of 760 au, and the deuterium mass was used for all hydrogens to allow for more efficient sampling.⁶⁰

2.2. Aggregation Simulations. Using the same basic ab initio molecular dynamics setup as described above, a series of aggregation simulations, $\text{HCl}(\text{H}_2\text{O})_{n-1} + \text{H}_2\text{O}$ (starting with $n = 1$), has been carried out according to the following general protocol that implements electrostatic steering in the initial encounter phase of the aggregating molecular species. In any aggregation step from $n - 1$ to n , the existing cluster composed of HCl and $n - 1$ water molecules and the added water molecule were initially oriented with aligned molecular dipole moments at a fixed distance from the oxygen of the added water molecule to the nearest heavy atom of the cluster. For that purpose, first the $n - 1$ cluster and a single water molecule were each separately rotated such that their dipole moment was parallel to some chosen space fixed axis. Subsequently, the center of mass of the $n - 1$ cluster was placed in the origin, whereas the center of mass of the additional water molecule was placed on the dipole-axis in either direction between 7 and 9 Å away from the origin, yielding two starting structures with a distance of nearest heavy

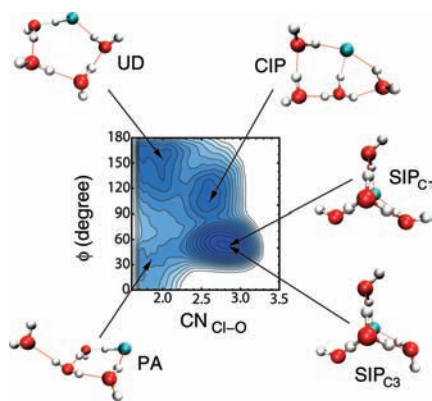


Figure 3. Free energy landscape of $\text{HCl}(\text{H}_2\text{O})_4$ for dissociation as a function of the two collective variables as defined in section 2.1. Contour lines of constant free energy are shown with a spacing of 2.5 kJ/mol. The locations of the minima are connected via arrows to the corresponding optimized structures.

atoms of about 5 and 7 Å. The heavy atom of the existing cluster nearest to the oxygen of the added water molecule can either be O or Cl and is uniquely determined by the initial structure.

Following these setup steps, the total system was then equilibrated in the canonical ensemble at 0.5 K while keeping the distance of the nearest heavy atom to the added water oxygen atom fixed in terms of a distance constraint; note that only this distance but neither the orientation nor any atom position were held fixed. To ensure stable integration of the equations of motion including this constraint, a smaller time step of 0.097 fs was used at this stage. The purpose of this constraint equilibration is not only to get properly thermalized fragments and initial conditions, but also to relax and thermalize the relative orientation of the fragments. After some equilibration period of typically 2 ps, initial conditions were sampled from such constrained canonical trajectories and subsequently propagated in the microcanonical ensemble in the range of typically 10–60 ps each without imposing the distance constraint again using the larger time step of 0.121 fs; note that the longest of these runs has been extended up to 95 ps. Thus, all atoms are allowed to move freely during this aggregation dynamics, and lowering the potential energy when sliding downhill on the global potential energy surface leads to an increase of kinetic energy.

On the basis of this protocol, nearly 50 such independent *ab initio* trajectories have been generated where the majority, about 35, have been sampled for the most important $n = 4$ case. Finally, we note that about 1 ns of such *ab initio* molecular dynamics runs in total was necessary to establish the ensemble of trajectories on which the following analysis is based.

3. RESULTS AND DISCUSSION

3.1. Traditional Dissociation Mechanism. Comprehensive mapping of the two-dimensional FES by *ab initio* metadynamics using the approach described in section 2.1 reveals that the surface to describe dissociation of $\text{HCl}(\text{H}_2\text{O})_4$ is characterized by three prominent minima as revealed by Figure 3. They are identified in the contour plot as the UD, CIP, and SIP species (see Figure 1), where in the latter case the two different conformers, $\text{SIP}_{\text{C}1}$ and $\text{SIP}_{\text{C}3}$, are close in energy and cannot be resolved by the chosen CVs. It should be stressed that no lower-lying direct pathway connecting UD to SIP via a single transition state could be found in our study; neither it is known from previous studies known to us. Thus, dissociation according

to the traditional mechanism is a two-step reaction passing through an intermediate CIP species, that is, $\text{UD} \rightarrow \text{CIP} \rightarrow \text{SIP}$.

On the basis of this procedure, a microscopic dissociation mechanism can be extracted from the simulations, which is illustrated in Figure 4. By starting from the UD local minimum, the first transition state, denoted as TS1, is formed by first distorting the originally nearly-planar, five-membered ring of the heavy atoms: the water molecule that donates a hydrogen bond to the HCl moves out of the plane toward the free hydrogen of the water receiving a hydrogen bond from HCl, while the Cl atom moves to the opposite side of the plane (see blue arrows). The hydrogen of HCl shifts to the hydrogen-bond-accepting water, thus forming hydronium, which now donates a hydrogen bond to the Cl anion. From this transition state TS1, the reaction proceeds toward CIP by breaking the hydrogen bond that the out-of-plane water molecule received from the next water in the ring. In its place, the out-of-plane water molecule accepts a hydrogen bond from the hydronium, to which it is sufficiently close due to the initial ring distortion in forming TS1. The water molecule, which lost its hydrogen bond acceptor, rotates to donate its initially free hydrogen to the Cl ion, thus completing the formation of the local minimum CIP, in which cation and anion, H_3O^+ and Cl^- , are in direct contact, generally referred to as a contact ion pair.⁶¹ The rupture of the hydrogen bond between Cl and the water molecule in the three-membered ring consisting of Cl, hydronium, and a water molecule allows the system to form the second transition state, TS2. From there, the formation of SIP follows through a series of rearrangements: One proton is transferred from the hydronium to the water molecule opposite the Cl ion in the four-membered ring consisting of two water molecules, one hydronium, and the Cl ion. This newly formed hydronium in turn flips its free hydrogen toward the water molecule that broke away from the Cl during the formation of TS2. The latter water molecule then re-forms a hydrogen bond with Cl. According to this rearrangement pathway, the proton stemming from the dissociated HCl molecule, marked in black in the figure, ends up in one of the intact water molecules. Importantly, this particular proton (or deuteron in case of using DCl instead) establishes one of the three accepted hydrogen bonds that solvate the Cl anion in the SIP species.

The next step of this part of the analysis consists of examining the relative free energies and, in particular, the free energy barriers along this dissociation pathway. There are three easily discernible minima in the FES as shown in Figure 3. The CIP minimum lies about 1.3 kJ/mol lower than the undissociated UD structure, while the saddle point between these two structures lies approximately 7.7 kJ/mol higher than UD. The CIP minimum itself is ~ 13.7 kJ/mol higher than the SIP global minimum structure, and the barrier between the two minima is of the order of 5.4 kJ/mol. A fourth minimum, labeled PA, can be found about 23.5 kJ/mol above the SIP global minimum with a low barrier toward SIP of roughly 1.2 kJ/mol.

Hydrogen bonds obviously play a crucial role in the energetic stabilization of such microsolvated HCl clusters. The isomerization reaction described previously takes place by changes in the hydrogen-bond topology (i.e., rupture and/or reorganization of some hydrogen bonds); it is therefore likely that the characterization of that topology and its change can be helpful to describe the course of the reaction. For this purpose, we identify a few hydrogen-bond descriptors, which convey the essence of each transformation: the number of hydrogen-bond donors, acceptors, and free hydrogen atoms. In this context, we talk about a

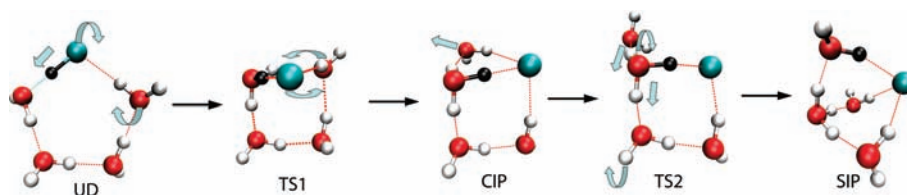


Figure 4. Traditional dissociation mechanism (schematic), UD \rightarrow TS1 \rightarrow CIP \rightarrow TS2 \rightarrow SIP, according to the free energy surface shown in Figure 3. The proton of HCl is marked in black to mark its position according to this dissociation pathway. Thick blue arrows serve as guides to the eye for visualizing how the structures reorganize to get to the next step on the path to dissociation.

Table 1. Hydrogen-Bond Descriptors Used To Characterize the Topology of All Structures as well as the Species Order Parameter P As Defined in Eq 2

	UD	TS1	CIP	TS2	SIP
number of hydrogen bonds					
from H ₂ O to Cl	1	1	2	1	3
from H ₃ O ⁺ to Cl	0	1	1	1	0
from HCl to O	1	0	0	0	0
from H ₂ O to O	3	2	1	1	0
from H ₃ O ⁺ to O	0	1	2	2	3
number of free H	4	4	3	4	3
order parameter P	28.0	48.0	36.2	27.1	31.0

hydrogen bond if the hydrogen–chlorine distance is between 1.5 and 2.5 Å or the hydrogen–oxygen distance is between 1.3 and 2.1 Å. We also require the O–H–O angle to be larger than 145° for hydrogen bonds. In Table 1, we report the values for these descriptors for both minima and transition states.

Passing from UD to TS1, the number of hydrogen bonds stays the same; just the character of several of them changes due to the formation of the Cl[−] and H₃O⁺ pair. There is one less water-donated hydrogen bond and no longer any HCl-donated bonds; instead the newly formed hydronium donates two hydrogen bonds, one to O and one to Cl. Even though the total number of hydrogen bonds remains constant, TS1 is higher in energy than UD because the chloride's negative charge is not sufficiently stabilized by two hydrogen bonds, and the donation from a third molecule is necessary. This happens in the step from TS1 to CIP, where the Cl anion accepts an additional hydrogen bond from a second water. Accordingly, the number of non-hydrogen-bonding, that is, free, hydrogen atoms decreases; additionally, one water-to-water hydrogen bond is broken, and a second hydronium-to-water hydrogen bond is formed.

The CIP and SIP structures both have the same total number of hydrogen bonds; the main difference is that in SIP all hydrogen bonds to Cl are donated by water molecules, each of them accepting a hydrogen bond from the hydronium, while in CIP one hydrogen bond to Cl comes directly from the hydronium. Also, the topology is quite different: the CIP species consists of a three-membered, hydrogen-bonded ring, consisting of Cl, one water molecule, and hydronium, as well as of a four-membered ring connecting Cl, hydronium, and two water molecules. The SIP topology features three equal four-membered rings formed by Cl, water, hydronium, and again water. Note that also the order of the parts in the four-membered rings of SIP is different from that in the single four-membered ring in CIP. The high energy gain in passing from CIP to SIP can be explained by the fact that, in SIP, the positive and negative charges are separated

and shielded by water, the hydrogen-bond angles are closer to ideal, in particular the unfavorable three-membered ring of CIP does not exist in SIP, and that a highly symmetrical structure is achieved in SIP. In fact, the transition state TS2 is formed from the CIP structure by eliminating the three-membered ring via a hydrogen-bond rupture between the Cl ion and the water molecule of that ring.

3.2. Aggregation-Induced Dissociation Mechanism. The traditional two-step dissociation mechanism via a partially dissociated intermediate, UD \rightarrow TS1 \rightarrow CIP \rightarrow TS2 \rightarrow SIP, as described above, certainly achieves in a most elegant way the significant changes that are necessary to convert the two-dimensional, ring-like hydrogen-bonded topology of UD into the three-dimensional, most compact Eigen-like motif underlying the SIP species according to Figure 4. However, the free energy barriers ΔF^\ddagger to be surmounted along this pathway are enormous, about 930 K for TS1 to reach CIP and another 650 K to reach SIP via TS2 from CIP, when compared to thermal energies $k_B T$ at temperatures of the order of 1 or 10 K. Thus, according to the standard theory of thermally activated reactions, the rate $\propto \exp[-\Delta F^\ddagger/k_B T]$ associated with both processes would be vanishingly small at such low temperatures. The unequivocal conclusion, at this stage, is that the molecular UD species, once it is formed at 1 K, is not expected to dissociate into the global SIP minimum in the sense of a thermal process at any reasonable rate. Similarly, the global SIP minimum cannot be reached thermally from the CIP intermediate either.

A very different mechanism of how SIP can be formed at temperatures as low as 1 K has been sketched in our previous short communication.⁵⁵ It goes back to the observation that a so-called partially aggregated (PA) structure, so far not discussed, has been found when sampling the FES in the two-dimensional space that hosts the reaction coordinate for dissociation of UD into SIP. This species manifests itself only by a shallow free energy minimum in the lower-left corner of the reaction subspace; see Figure 3. The barrier from PA to SIP is quite shallow and could only be roughly estimated; it is found to be smaller than about 140 K. Optimization of the PA structure shows that it is best conceived as an undissociated, cyclic heteromolecular HCl/water tetramer, HCl-(H₂O)₃, where a fourth water molecule is loosely attached by accepting a hydrogen bond from the remaining dangling OH group of the central water molecule, that is, HCl(H₂O)₃···H₂O according to Figure 1.

This observation opens up an alternate avenue to dissociation: instead of starting from the fully relaxed UD structure and trying to find low-energy pathways toward SIP, the existence of PA suggests that dissociation might occur readily when letting HCl(H₂O)₃ react with the fourth water molecule. To scrutinize this scenario, the protocol described in section 2.2 has been devised to launch a set of aggregation simulations that mimic

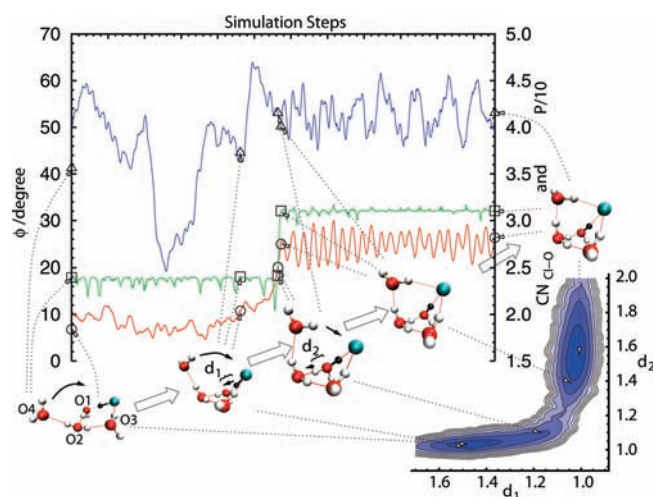


Figure 5. Formation of SIP out of the PA precursor species according to the aggregation-induced dissociation mechanism: representative snapshots of the configurations from one typical trajectory are shown together with the evolution of the two collective variables (CVs) and the order parameter (P), all defined in the text, as a function of the number of simulation steps. The blue line together with the left scale shows the dihedral angle ϕ , while the right scale corresponds to both the coordination number CN_{Cl-O} (red line) and P rescaled by $1/10$ (green line). Solid arrows indicate reorientation of atoms to get to the next step in the snapshot sequence, and the proton originating from HCl is marked in black throughout the reaction sequence. Also shown is a contour plot of the negative logarithm of the probability density sampled during the simulations as a function of two selected O–H distances, d_1 and d_2 , as defined in the snapshots. Dotted arrows indicate the position of the selected snapshots in the evolution of the CVs as well as their position in the contour plot.

dynamically what happens if an additional water molecule gets attracted by the undissociated $HCl(H_2O)_3$ species.

The statistical sample of about 35 independent trajectories probing aggregation of $HCl(H_2O)_3$ with the fourth H_2O allows for a qualitative analysis of the $n = 4$ scenario as follows: (i) approach of the existing cyclic $HCl(H_2O)_3$ cluster from the Cl side predominantly yields the contact ion pair species CIP, but also SIP and another compact CIP-like structure, CIP_2 , to be discussed below; (ii) the two different constraint distances for the approach from the O side do yield the same scenario as follows; (iii) approach of the existing cyclic $HCl(H_2O)_3$ cluster from the O side always yields first the partially aggregated PA species, which then reacts further to produce the solvent-shared ion pair SIP or undissociated UD, whereas the CIP structure is never observed upon approach from the O side; a PA-like structure with the last water attached not to the central water of the four-membered ring, but to either of the other water molecules, is more likely to yield the CIP structure, because then the three-membered ring of hydronium, Cl, and water that is necessary for the CIP structure can be readily formed, whereas in the PA structure the singly attached water would first have to migrate to such a position; (iv) the UD and CIP structures, once generated, were never observed to convert into PA or SIP species; however, in one case, the CIP structure converted later into CIP_2 ; and (v) the proton stemming from dissociation of HCl (marked in black in the figures) is found in one of the intact water molecules but never in the hydronium core concerning the SIP structure.

Having qualitatively discussed the phenomenon as such, only detailed structural analyses of the underlying dynamical trajectories

can yield the full picture. To ease the discussion, the oxygen atoms in the initial structure are labeled as follows: O1 initially receives a hydrogen bond from HCl, the water molecule with O2 both receives and donates a hydrogen bond to the other two water molecules, while the water with O3 initially donates a hydrogen bond to Cl, and finally the oxygen O4 belongs to the incoming water according to Figure 5. In addition to the two CVs defined previously, we introduce here an order parameter to quickly distinguish between species:

$$P = \text{perm}(M_{i,j}) = \sum_{\mathcal{P}} \prod_i M_{i,\mathcal{P}_i} \quad (2)$$

with the 5×5 matrix M encoding the hydrogen-bonding pattern between the five heavy atoms as follows:

$$M_{i,j \neq i} = M_{j,i} = \sum_H (v_{i,j} + v_{j,i} - v_{i,j}v_{j,i}) \quad (3)$$

The values v_{ij} are a continuous measure of the heavy atom X_i donating a specific H to the other heavy atom X_j :

$$v_{i,j} = [(1 + (R_{H,X_i}/B_{X_i})^k)(1 + (R_{H,X_j}/A_{X_j})^k)]^{-1} \quad (4)$$

where the exponent $k = 40$, the cutoff parameters $B_O = 1.3 \text{ \AA}$, $B_{Cl} = 1.9 \text{ \AA}$, $A_O = 2.3 \text{ \AA}$, and $A_{Cl} = 2.7 \text{ \AA}$, and R_{H,X_i} is the distance of the heavy atom X_i to the specific hydrogen atom H currently being considered in the sum in eq 3. Thus, if there is a hydrogen bond between heavy atoms X_i and X_j , the corresponding matrix element $M_{i,j}$ is close to unity, whereas it is close to zero otherwise. Note that $v_{i,j}$ is different from the purely boolean definition of hydrogen bonds used in the previous section. The diagonal elements $M_{i,i}$ are set to 4 if $X_i = Cl$ and to 1 for the case of oxygen.

On the basis of these descriptors, we can now deduce the aggregation-induced dissociation mechanism that leads to the global minimum structure, SIP, as a result of forming the partially aggregated PA precursor species, $HCl(H_2O)_3 \cdots H_2O$, obtained by adding the fourth water molecule to the heteromolecular $HCl(H_2O)_3$ cycle. In the trajectories where the fourth water molecule attacks from the O side, the PA intermediate is always formed first by accepting a hydrogen bond from O2, which is the closest water molecule in this case due to this dipole-steered pre-orientation; see Figure 5 and the atom labeling introduced therein to follow this discussion. The singly attached water molecule approaches the Cl atom, while the original four-membered ring folds along the O1–O3 axis as schematically illustrated in Figure 5. When one hydrogen of O4 gets close enough to the Cl, the already unusually symmetric hydrogen bond of HCl to O1 shifts the hydrogen fully toward O1, thus forming hydronium upon completing proton transfer. As soon as Cl is fully solvated by accepting three hydrogen bonds, the hydrogen between O1 and O2 moves toward O2, thus arriving at the dissociated SIP local minimum species. Note that, although these different steps are typically observed in roughly this sequence, we do not imply here a strictly stepwise mechanism in view of the rather significant kinetic energy that is available within the molecular complex after aggregation. However, the contour plots of two O–H distance phase space densities during the aggregation simulations also depicted in Figure 5 clearly support the above sequence of the hydrogen-bond reorganization.

Upon the initial formation of the PA structure, the singly attached water is still quite flexible and has a lot of kinetic energy, which can be “used” in a manner alternative to forming the dissociated SIP species. It is observed in some of the trajectories

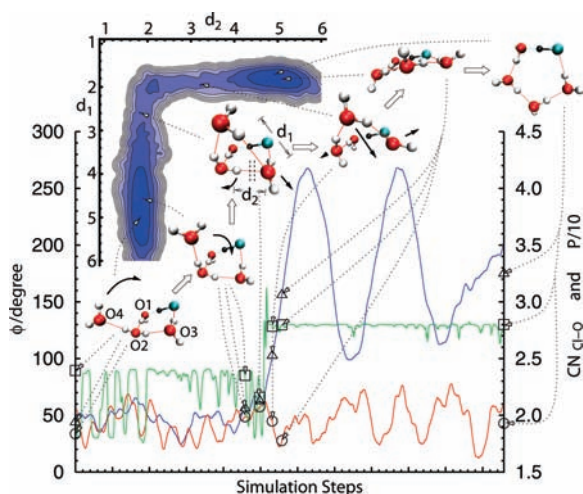


Figure 6. Formation of UD out of the PA precursor species; see caption of Figure 5 for symbols and labeling.

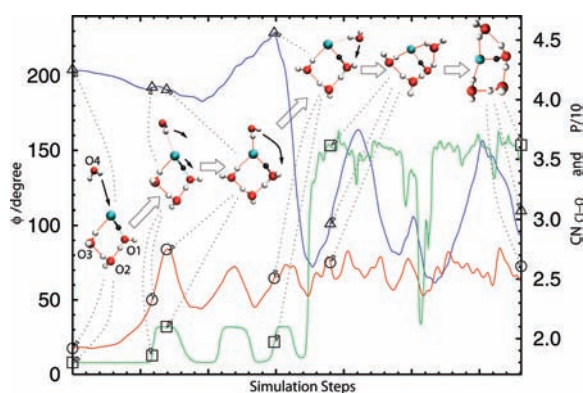


Figure 7. Formation of CIP from the approach of the additional water from the Cl side; see caption of Figure 5 for symbols and labeling (probability density not shown).

that the undissociated UD structure is formed where O4 is seen to first donate an additional hydrogen bond to O3. When this bond is formed, the original hydrogen bond between O2 and O3 breaks, yielding a distorted five-membered ring, which then just needs to expand to flatten out toward the UD structure. This mechanism is illustrated in greater detail in Figure 6.

Thus, both dissociated and undissociated species, SIP and UD, can be formed upon dipole-steered attack of cyclic $\text{HCl}(\text{H}_2\text{O})_3$ by the fourth water molecule from the O side. In those trajectories where the additional water O4 approaches instead from the Cl side in a dipolar pre-orientation, a hydrogen bond is first formed between the incoming water and Cl, while the proton of HCl is transferred to O1, yielding the contact ion pair motif that characterizes the partially dissociated CIP structure according to Figure 7. Next, without losing sight of the Cl ion, the water O4 moves in a second step toward the hydronium O1. Because of the large kinetic energy still in the system during these events, it is hard to tell whether the hydrogen bond to the Cl is broken and later re-formed during this movement or whether this hydrogen bond stays intact during that sequence of events. However, once O4 is close enough to O1, a stable hydrogen bond between the water O4 and hydronium O1 is formed, and the hydrogen bond between O4 and Cl settles. This mechanism is depicted in more detail in Figure 7.

In one of the trajectories with water approaching from the Cl side, the free hydrogen of the hydronium O1 pointed away from O4 in the second step, and in that case the free hydrogen of O2 was closer to O4 than usual. Even though the free hydrogen of O2 was initially still farther away, the original four-membered ring, consisting of Cl–O1–O2–O3, distorted enough in addition to movement of O4 toward that hydrogen such that a hydrogen bond was established. When that happened, the hydronium O1 transferred a proton to O2, thus yielding the system in the SIP global minimum instead of the CIP species that is usually observed for that particular attack. Because this was only observed once, the general relevance of this mechanism for forming SIP from this approach direction is unknown, but it is certainly a feasible pathway to full dissociation due to aggregating one more water molecule to $\text{HCl}(\text{H}_2\text{O})_3$.

Finally, one other trajectory was found, which first yielded a CIP structure as described above; however, due to fluctuations O4 also came close to O3 and the hydrogen bond of O4 to Cl broke, and the O4 water molecule rotated to donate the freed hydrogen to O3, thus yielding a thus far unknown stable structure of a very compact contact ion pair denoted CIP₂ and depicted in Figure 1. The topology of this structure is rather similar to that of the SIP minimum in that just the Cl is swapped with one of the water molecules in SIP.

Up to this point, only the last step that leads to dissociation from $\text{HCl}(\text{H}_2\text{O})_3$ via $\text{HCl}(\text{H}_2\text{O})_3 \cdots \text{H}_2\text{O}$ to $\text{H}_3\text{O}^+(\text{H}_2\text{O})_3\text{Cl}^-$ and some “side reactions” have been analyzed. The question, however, remains whether or not the cyclic heterotetramer, that is, $\text{HCl}(\text{H}_2\text{O})_3$ itself, can be produced via aggregation of HCl with water molecules, one by one. Indeed, the aggregation simulations show that this is readily possible, using the same protocol as before. Starting with HCl and one H_2O yields the undissociated heterodimer, $\text{HCl}(\text{H}_2\text{O})$, in its lowest-energy structure where HCl is the hydrogen-bond donor as shown in Figure 8. Two distinct but similar pathways have been observed, which both yield the same global minimum product.

The same is true for the second aggregation step once $\text{HCl}(\text{H}_2\text{O})$ is used to serve as the nucleus for attaching a second water molecule; see again Figure 8. Here, aggregation results first in a linear chain of the three molecules. Again, two pathways have been observed in the simulations as depicted where the intermediate linear arrangement contains the HCl molecule either at the center or as one of the termini. Fluctuations due to the large kinetic energy gained upon this aggregation step, $\text{HCl}(\text{H}_2\text{O}) + \text{H}_2\text{O} \rightarrow \text{HCl}(\text{H}_2\text{O})_2$, cause the chain to bend significantly. Eventually the ends of the chain can meet, thus forming an undissociated ring-like heterotrimer, $\text{HCl}(\text{H}_2\text{O})_2$. As the kinetic energy in such a small system is only slowly distributed equally in all degrees of freedom, this ring-like structure can reopen and close several times within one simulation. Once the energy dissipates, the ring-like structure predominates because it is the global minimum on that PES.

Having now a ring-like cyclic structure to start with, the next step yields the cyclic $\text{HCl}(\text{H}_2\text{O})_3$ species by two interesting ring insertion mechanisms; see Figure 8. In the case that the approaching water forms a hydrogen bond to the water molecule, which already donates a hydrogen bond to Cl, the incoming water simply approaches Cl without losing its initial hydrogen bond from the cluster. Once it is close enough, it donates a hydrogen bond to Cl, while the hydrogen bond from the other water molecule to Cl is broken. The mechanism is more complex when the approaching water molecule first forms a hydrogen

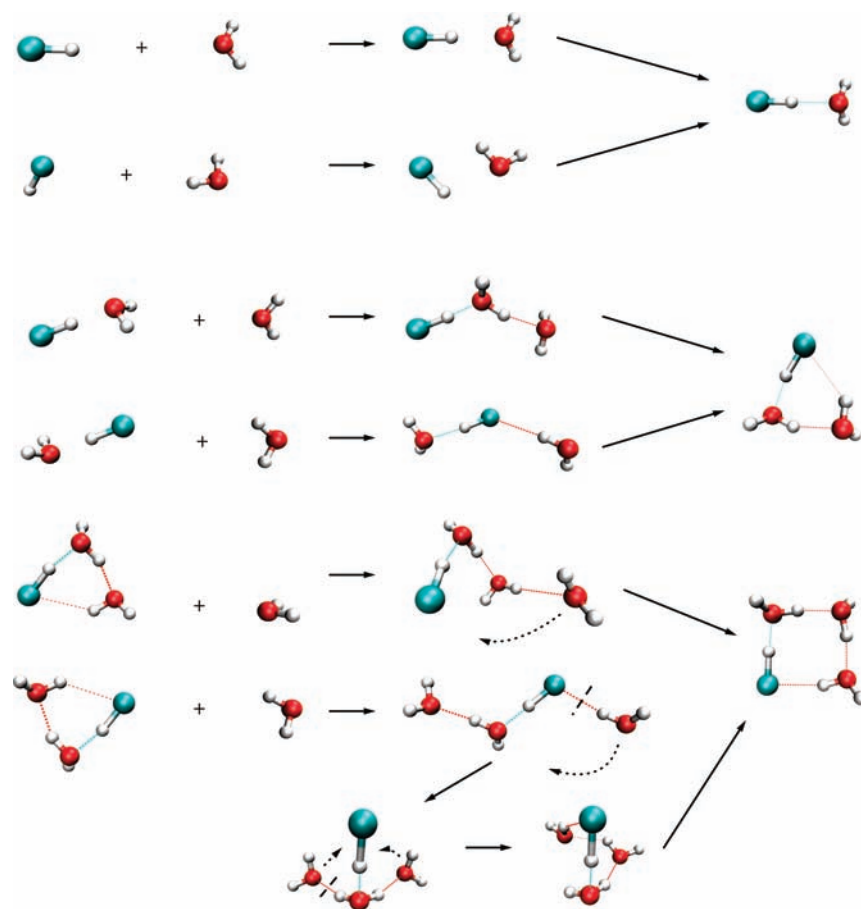


Figure 8. Stepwise aggregation mechanism of HCl with three water molecules forming cyclic heteromolecular species: $\text{HCl} + 3\text{H}_2\text{O} \rightarrow \text{HCl}(\text{H}_2\text{O}) + 2\text{H}_2\text{O} \rightarrow \text{HCl}(\text{H}_2\text{O})_2 + \text{H}_2\text{O} \rightarrow \text{HCl}(\text{H}_2\text{O})_3$. The dotted arrows serve as guides to the eye for visualizing how the structures reorganize to get to the next step on the path to dissociation, while the solid arrows define the sequence of steps along the path. Hydrogen-bond breaking events are indicated by dashed lines where non-obvious.

bond to Cl, as is the case from the other initial electrostatic steering condition. When this bond is formed, the other water donating a hydrogen bond to Cl breaks its bond to Cl, resulting in a chain-like zigzag structure. The original incoming water then moves toward the water molecule that receives a hydrogen bond from Cl and receives a hydrogen bond from that water while breaking the bond to Cl. Next, the third water moves toward Cl, and the originally incoming water, while breaking its bond from the central water, thus donates a hydrogen bond to Cl and accepts a hydrogen bond from the originally incoming water molecule. The cluster then has the right connectivity, but is distorted and flattens out in the final step. Both of these pathways for the formation of the $n = 3$ cluster are also visualized in Figure 8. It should be stressed that these observations are based on a quite limited number of trajectories; even richer aggregation scenarios might be found when using a larger ensemble of such independent aggregation simulations.

3.3. Discussion: Aggregation-Induced Reactions. In summary, the stepwise aggregation simulations $\text{HCl}(\text{H}_2\text{O})_{n-1} + \text{H}_2\text{O}$ starting with $n = 1$ and ending with $n = 4$ as reported in section 3.2 lead to a dissociation mechanism, which is distinctly different from the traditional one observed upon dissociating HCl within the size-selected $\text{HCl}(\text{H}_2\text{O})_4$ cluster. In particular, here are the prominent characteristic features of the aggregation-induced dissociation scenario illustrated in Figure 2 that

produces the SIP species, which is the most stable structure: (i) a sequence of aggregation simulations using electrostatic steering initial conditions results in successive growth of undissociated clusters $\text{HCl}(\text{H}_2\text{O})_n$ by adding one water molecule after the other up to forming the heterocyclic $n = 3$ tetramer species; (ii) adding the critical fourth water molecule to this $\text{HCl}(\text{H}_2\text{O})_3$ species produces, upon approaching it from the O side according to dipolar pre-orientation, a precursor state, which is the PA structure $\text{HCl}(\text{H}_2\text{O})_3 \cdots \text{H}_2\text{O}$, for the dissociation reaction; and (iii) it is this undissociated PA species that readily dissociates into the SIP structure upon using kinetic energy obtained by converting the binding energy gained due to aggregation into kinetic energy, thus leading to athermal fluctuations that aid in surmounting the remaining energy barriers. It should be noted that other pathways exist such that the UD structure can also be formed out of the PA species in some cases and that CIP can be obtained when the incoming water molecule approaches the Cl side of the cyclic $\text{HCl}(\text{H}_2\text{O})_3$ cluster in dipolar steering orientation, and a novel, more compact contact ion pair, CIP₂, has been generated upon aggregation. Along the same lines of creating molecular diversity, two distinct aggregation pathways have been found for each step of the build-up sequence that yields the cyclic heterotetramer, $\text{HCl} + 3\text{H}_2\text{O} \rightarrow \text{HCl}(\text{H}_2\text{O}) + 2\text{H}_2\text{O} \rightarrow \text{HCl}(\text{H}_2\text{O})_2 + \text{H}_2\text{O} \rightarrow \text{HCl}(\text{H}_2\text{O})_3$, and it is expected that further such pathways also exist. Overall, the

stepwise aggregation approach is seen to provide a rich and interconnected network to cluster formation.

An important aspect is that the aggregating reactants, that is, the preformed $\text{HCl}(\text{H}_2\text{O})_n$ cluster and the approaching H_2O molecule, are both cooled to superfluid helium temperatures, that is, below 1 K, before their encounter. This is a reasonable assumption in view of the energy relaxation time of approximately 10^{-11} s of ref 71 in conjunction with encounter (recombination) times of the order of 10^{-10} to 10^{-8} s due to the bare dispersion attraction.⁷² Thus, the reactants are cooled from ambient to superfluid helium temperatures in the order of 10^{-11} s, which is on average much faster than encountering any aggregation partner on the associated time scales of at most 10^{-9} s. It should be noted that in this discussion we used the energy relaxation time given in appendix B of ref 71 instead of their cooling rate. This seems more appropriate, because in their case the energy is more than an order of magnitude higher, and the helium cluster explosively evaporates and leaves only a partially cooled, bare molecule behind.

The second key ingredient is the assumption that, at ultracold temperatures, not all of the potential energy released upon aggregation and binding in terms of kinetic energy is efficiently quenched by the superfluid helium environment. A large potential energy gain between the reactants being far apart and the aggregation product occurs for the step involving the formation of PA, and amounts to about 22 kJ/mol, corresponding to a thermal energy of about $2600 k_B K$. The time scale for the process of dissociation from PA to SIP is on the order of only 1–10 ps. Because the above-mentioned energy relaxation rate is at the upper limit of this time range, it can be assumed that the gained kinetic energy of several thousand kelvin cannot be fully quenched by the environment on the required ultrafast time scale. This implies that the system still has enough energy from forming the first hydrogen bond (i.e., $\text{HCl}(\text{H}_2\text{O})_3 + \text{H}_2\text{O} \rightarrow \text{PA}$) to overcome the barrier from PA to SIP, although the energy released from previous aggregation steps up to forming $\text{HCl}(\text{H}_2\text{O})_3$ has already been dissipated even before PA is formed, in view of the separation of time scales. Thus, a crucial ingredient in such aggregation-induced reactions is the idea that the remaining kinetic energy can be “used” to overcome sufficiently small barriers that might still exist between precursor and final states, such as the PA and SIP species in the present case. This scenario is what has been termed “aggregation-induced dissociation”.⁵⁵

Clearly, it is to be expected that not every encounter event leads to the minimum energy structure for the given cluster size n . Indeed, trajectories have been observed that end up in the molecular UD structure and the dissociated CIP structure for $n = 4$, as described above in more detail. Even an unexpected novel minimum structure, CIP_2 , could be obtained following the aggregation simulation protocol. According to the proposed scenario of aggregation-induced dissociation, the UD, CIP, and CIP_2 species would be unreactive trap states that are not expected to dissociate into SIP for the reasons presented as a result of the FES analysis in section 3.1, that is, essentially exceedingly large energy barriers on the scale of the available thermal energy at sub-kelvin temperatures. Finally, metastable, non-equilibrium structures of smaller clusters are also expected to be formed as a result of aggregation, which, however, we did not observe so far. Comprehensive exploration of these and other alternate pathways is certainly interesting, but constructing such an “aggregation ensemble” as a function of n is certainly beyond

the scope of this first investigation into aggregation-induced reactions.

Turning our attention from microsolvation to bulk solvation in the liquid state, the aggregation-induced dissociation mechanism found within our finite cluster setup corresponds to an indirect, “solvent-mediated” proton transfer mechanism from HCl to H_3O^+ via other water molecules that are used as proton-transfer bridges, in the sense of Grotthuss-like structural diffusion.⁴ This implies that the additional proton that is necessary to create the hydronium cation, H_3O^+ , is not provided by the acid, HCl, according to the mechanism shown in Figure 5 where the “acidic proton” (or deuteron) is marked in black. Thus, using DCI instead of HCl does not lead to a H_2DO^+ species in the first place. Clearly, in microsolvation clusters, which are rigid at ultralow temperatures, the position of the “acidic proton” becomes topologically fixed at one of the three solvating water molecules that are shared by both anion and cation in the SIP species. This is in stark contrast to bulk solvation where all protons eventually become equivalent after Grotthuss diffusion (except for isotope effects).

Before closing the discussion of aggregation-induced reactions, let us compare this concept to related ideas presented in earlier work. In the context of “very low temperature” synthesis of molecules at temperatures down to 10 K, as relevant, for example, to chemistry occurring inside dense interstellar clouds, interesting reaction scenarios have been revealed.^{73–77} In the context of these so-called “chemical activation” mechanisms, the energy released in a primary reaction is utilized to surmount a barrier for a subsequent reaction. However, these covalent reactions are studied in the gas phase, that is, effectively in a vacuum, whereas a solvating environment interacts with the aggregating species in the present case, which, themselves, interact via hydrogen bonding. Furthermore, the temperature in superfluid helium nanodroplets is in the sub-kelvin range, which is an order of magnitude lower, implying that only reactions with barriers that are also an order of magnitude smaller can reasonably be expected to occur thermally.

The fundamental idea of “successive capture and coagulation of atoms and molecules to small clusters in large liquid helium clusters”⁷² has already been spelled out early on in ref 72 without, however, considering the possibility that this process can open up novel, aggregation-induced, low-energy pathways to chemical reactions as explored herein. The idea of successive capture and coagulation⁷² has been confirmed in an extensive study of the growth of homomolecular water clusters in superfluid helium droplets where the formation of large cyclic structures up to the hexamer has been found.⁷⁸ Interestingly, insertion of individual water molecules into preformed cyclic water oligomers has been observed from mostly static PES mappings⁷⁸ much alike to what we have found here from dynamical aggregation simulations for heteromolecular HCl/water clusters up to the undissociated tetramer. Surmounting low-energy barriers has been ascribed in that study⁷⁸ to thermal activation at the sub-kelvin temperature of helium droplet experiments, in addition to finding that zero-point fluctuations are significant in facilitating or enabling these processes. In a similar study⁷⁹ of $(\text{HF})_n$ clusters in helium droplets, cyclic structures were only found up to $n = 4$, while upon adding one more HF the barrier to the cyclic $n = 5$ global minimum could no longer be surmounted, leaving the system in a PA-like “4 + 1” structure. In aggregation-induced reactions, a key concept is that potential energy, that is, the binding energy gained upon adduct formation, gets converted into kinetic energy

in view of “fast” aggregation versus “slow” cooling processes, which in turn helps to overcome barriers due to the thereby increased athermal fluctuations according to Figure 2. Finally, another ingredient is electrostatic steering during the initial phase of the aggregation process, which has been shown earlier to lead to non-covalent species diversity, thus explaining the formation of metastable molecular aggregates, as found, for example, in matrix isolation spectroscopy and helium environments, if temperature is sufficiently low;^{80,81} again, our key issue of enabling chemical reactions due to the aggregation process itself including the formation of reactive (i.e., “activated”) precursor states has not been addressed.

4. CONCLUSIONS AND OUTLOOK

The dissociation of acids in microsolvation environments is usually studied computationally by locating the minimum energy pathway that connects the most stable undissociated, molecular species to the lowest-energy dissociated, (zwitter)ionic structure, given a certain fixed number of solvent molecules. If the dissociated species is lower in energy relative to the most stable undissociated structure for a given number n of solvent molecules, it is said that n solvent molecules are required to establish dissociation in a microsolvation setup. In the case of HCl interacting with water molecules, a number of $n = 4$ solvent molecules is needed to stabilize the fully dissociated state, $\text{H}_3\text{O}^+(\text{H}_2\text{O})_3\text{Cl}^-$, being a solvent-shared ion pair. The energy barriers, however, that connect the (metastable) undissociated with the (most stable) dissociated state via an intermediate turn out to be insurmountably high at ultralow temperatures, as encountered, for example, in superfluid helium nanodroplets now used to study microsolvation.

In stark contrast to this approach, we pose here the question of what happens if, instead of starting with n solvent molecules around the undissociated Brønsted acid, rather, one adds one solvent molecule after the other, thereby producing a growing cluster, until the acid gives away its proton to a hydrogen-bonded water molecule. This question is highly relevant to the process of successive capture and subsequent stepwise aggregation of molecules inside large helium droplets using the pickup technique in helium nanodroplet isolation (HENDI) spectroscopy. Upon aggregating a single HCl molecule with a growing number of water molecules, one by one, it is observed that the undissociated ring-like structure grows up to $n = 3$, that is, up to the cyclic $\text{HCl}(\text{H}_2\text{O})_3$ heterotetramer, where the step $\text{HCl}(\text{H}_2\text{O})_2 + \text{H}_2\text{O} \rightarrow \text{HCl}(\text{H}_2\text{O})_3$ occurs via interesting ring insertion mechanisms. When adding the fourth water molecule, a partially aggregated undissociated structure $\text{HCl}(\text{H}_2\text{O})_3 \cdots \text{H}_2\text{O}$ is obtained, where the added water molecule accepts a hydrogen bond from the cyclic four-membered $\text{HCl}(\text{H}_2\text{O})_3$ ring. This species can be viewed as an activated precursor species where the HCl molecule readily dissociates, thus yielding the reaction product, that is, a fully dissociated solvent-shared ion pair. The potential energy profile along the pathway involving the precursor species to the product is essentially downhill. Remaining energy barriers, being about an order of magnitude smaller than those involved when transforming the undissociated $n = 4$ equilibrium structure straightforwardly into the product, can be easily overcome by using kinetic energy released when forming the hydrogen bond that leads to the precursor state. Thus, the necessary energy for the reactive last step, according to this mechanism, comes from converting potential energy released as a result of aggregation

into kinetic energy. This activation, therefore, is not ruled by thermal equilibrium but stems from athermal, non-equilibrium dynamics. Taken together, these key ingredients define what we call “aggregation-induced chemical reactions”.

Beyond the specific case, the general concept of aggregation-induced chemical reactions might be another avenue to enable chemistry at very low temperatures, where quantum-mechanical tunneling, photochemical excitations, and the like are usually invoked to explain unexpected products and unusual reactivities. This is a subject that is currently under investigation in Bochum both theoretically and experimentally.

■ ASSOCIATED CONTENT

Supporting Information. Optimized structures and energies. This material is available free of charge via the Internet at <http://pubs.acs.org>.

■ AUTHOR INFORMATION

Corresponding Author

harald.forbert@theochem.rub.de

Present Addresses

[†]Dipartimento di Chimica, Università degli Studi di Sassari, Istituto Officina dei Materiali del CNR, UOS SLACS, Via Vienna 2, 07100 Sassari, Italy.

[‡]Faculty of Chemistry, Nicolaus Copernicus University, Gagarina 7, 87-100 Toruń, Poland.

[§]Department of Chemistry, Indian Institute of Technology Kanpur, Kanpur 208016, India.

■ ACKNOWLEDGMENT

We thank Martina Havenith and her helium spectroscopy group, in particular Gerhard Schwaab and Anna Gutberlet, for a fruitful and pleasant collaboration on the subject. The work has been partially funded by the Deutsche Forschungsgemeinschaft (DFG MA 1547/8) within the framework of Forschergruppe FOR 618 on “Molecular Aggregation” and by Research Department “Interfacial Systems Chemistry” (RD IFSC) at RUB. Fonds der Chemischen Industrie (FCI) is gratefully acknowledged for general funding of D.M., and the simulations have been carried out using resources from Bovilab@RUB and Rechnerverbund-NRW (LiDo).

■ REFERENCES

- (1) Eigen, M. *Angew. Chem., Int. Ed. Engl.* **1964**, *3*, 1.
- (2) Elsaesser, T.; Bakker, H. J., Eds. *Ultrafast Hydrogen Bonding Dynamics and Proton Transfer Processes in the Condensed Phase*; Kluwer: Dordrecht, 2002.
- (3) Stillinger, F. H. In *Theoretical Chemistry: Advances and Perspectives*; Eyring, H., Henderson, D., Eds.; Academic Press: New York, 1978; pp 177–234.
- (4) Marx, D. *ChemPhysChem* **2006**, *7*, 1848. Addendum: *ChemPhysChem* **2007**, *8*, 209.
- (5) Rini, M.; Magnes, B. Z.; Pines, E.; Nibbering, E. T. J. *Science* **2003**, *301*, 349.
- (6) Woutersen, S.; Bakker, H. J. *Phys. Rev. Lett.* **2006**, *96*, 138305.
- (7) Mohammed, O. F.; Pines, D.; Nibbering, E. T. J.; Pines, E. *Angew. Chem., Int. Ed.* **2007**, *46*, 1458.
- (8) Tielrooij, K. J.; Timmer, R. L. A.; Bakker, H. J.; Bonn, M. *Phys. Rev. Lett.* **2009**, *102*, 198303.
- (9) Laasonen, K.; Klein, M. L. *J. Am. Chem. Soc.* **1994**, *116*, 11620.

- (10) Ando, K.; Hynes, J. T. *J. Mol. Liq.* **1995**, *64*, 25.
- (11) Ando, K.; Hynes, J. T. *J. Phys. Chem. B* **1997**, *101*, 10464.
- (12) Laasonen, K. E.; Klein, M. L. *J. Phys. Chem. A* **1997**, *101*, 98.
- (13) Ando, K.; Hynes, J. T. *Adv. Chem. Phys.* **1999**, *110*, 381.
- (14) Sillanpää, A. J.; Simon, C.; Klein, M. L.; Laasonen, K. *J. Phys. Chem. B* **2002**, *106*, 11315.
- (15) Ifimie, R.; Tuckerman, M. E. *Angew. Chem., Int. Ed.* **2006**, *45*, 1144.
- (16) Heuft, J. M.; Meijer, E. J. *Phys. Chem. Chem. Phys.* **2006**, *8*, 3116.
- (17) Ifimie, R.; Thomas, V.; Plessis, S.; Marchand, P.; Ayotte, P. *J. Am. Chem. Soc.* **2008**, *130*, 5901.
- (18) Packer, M. J.; Clary, D. C. *J. Phys. Chem.* **1995**, *99*, 14323.
- (19) Buesnel, R.; Hillier, I. H.; Masters, A. J. *Chem. Phys. Lett.* **1995**, *247*, 391.
- (20) Lee, C. T.; Sosa, C.; Planas, M.; Novoa, J. J. *J. Chem. Phys.* **1996**, *104*, 7081.
- (21) Planas, M.; Lee, C.; Novoa, J. J. *J. Phys. Chem.* **1996**, *100*, 16495.
- (22) Re, S.; Osamura, Y.; Suzuki, Y.; Schaefer, H. F., III. *J. Chem. Phys.* **1998**, *109*, 973.
- (23) Babelo, D. E.; Binning, R. C., Jr.; Ishikawa, Y. *J. Phys. Chem. A* **1999**, *103*, 4631.
- (24) Re, S.; Osamura, Y.; Morokuma, K. *J. Phys. Chem. A* **1999**, *103*, 3535.
- (25) Conley, C.; Tao, F. M. *Chem. Phys. Lett.* **1999**, *301*, 29.
- (26) Gertner, B. J.; Peslherbe, G. H.; Hynes, J. T. *Isr. J. Chem.* **1999**, *39*, 273.
- (27) Smith, A.; Vincent, M. A.; Hillier, I. H. *J. Phys. Chem. A* **1999**, *103*, 1132.
- (28) Elola, M. D.; Marceca, E. J.; Laria, D.; Estrin, D. A. *Chem. Phys. Lett.* **2000**, *326*, 509.
- (29) Milet, A.; Struniewicz, C.; Moszynski, R.; Wormer, P. E. S. *J. Chem. Phys.* **2001**, *115*, 349.
- (30) Re, S. *J. Phys. Chem. A* **2001**, *105*, 9725.
- (31) Chaban, G. M.; Gerber, R. B.; Janda, K. C. *J. Phys. Chem. A* **2001**, *105*, 8323.
- (32) Cabaleiro-Lago, E. M.; Hermida-Ramón, J. M.; Rodríguez-Otero, J. J. *J. Chem. Phys.* **2002**, *117*, 3160.
- (33) Tachikawa, M. *Mol. Phys.* **2002**, *100*, 881.
- (34) Voegelé, A. F.; Liedl, K. R. *Angew. Chem., Int. Ed.* **2003**, *42*, 2114.
- (35) Odde, S.; Mhin, B. J.; Lee, S.; Lee, H. M.; Kim, K. S. *J. Chem. Phys.* **2004**, *120*, 9524.
- (36) Kuo, J. L.; Klein, M. L. *J. Chem. Phys.* **2004**, *120*, 4690.
- (37) Goursot, A.; Fischer, G.; Lovallo, C. C.; Salahub, D. R. *Theor. Chem. Acc.* **2005**, *114*, 115.
- (38) Bianco, R.; Hynes, J. T. *Acc. Chem. Res.* **2006**, *39*, 159.
- (39) Odde, S.; Mhin, B. J.; Lee, K. H.; Lee, H. M.; Tarakeshwar, P.; Kim, K. S. *J. Phys. Chem. A* **2006**, *110*, 7918.
- (40) Lee, H. M.; Odde, S.; Mhin, B. J.; Suh, S. B.; Kim, K. S. *Mol. Phys.* **2007**, *105*, 2577.
- (41) Ndongmouo, U. F. T.; Lee, M.-S.; Rousseau, R.; Baletto, F.; Scandolo, S. *J. Phys. Chem. A* **2007**, *111*, 12810.
- (42) Masia, M.; Forbert, H.; Marx, D. *J. Phys. Chem. A* **2007**, *111*, 12181.
- (43) Xie, Z. Z.; Ong, Y. S.; Kuo, J. L. *Chem. Phys. Lett.* **2008**, *453*, 13.
- (44) Takayanagi, T.; Takahashi, K.; Kakizaki, A.; Shiga, M.; Tachikawa, M. *Chem. Phys.* **2009**, *358*, 196.
- (45) Weimann, M.; Fárnik, M.; Suhm, M. A. *Phys. Chem. Chem. Phys.* **2002**, *4*, 3933.
- (46) Hurlley, S. M.; Dermota, T. E.; Hydutsky, D. P.; Castleman, A. W., Jr. *Science* **2002**, *298*, 202.
- (47) Robertson, W. H.; Johnson, M. A. *Science* **2002**, *298*, 69.
- (48) Hurlley, S. M.; Dermota, T. E.; Hydutsky, D. P.; Castleman, A. W., Jr. *J. Chem. Phys.* **2003**, *118*, 9272.
- (49) Fárnik, M.; Weimann, M.; Suhm, M. A. *J. Chem. Phys.* **2003**, *118*, 10120.
- (50) Huneycutt, A. J.; Stickland, R. J.; Hellberg, F.; Saykally, R. J. *J. Chem. Phys.* **2003**, *118*, 1221.
- (51) Ortlieb, M.; Birer, Ö.; Letzner, M.; Schwaab, G. W.; Havenith, M. *J. Phys. Chem. A* **2007**, *111*, 12192.
- (52) Skvortsov, D.; Lee, S. J.; Choi, M. Y.; Vilesov, A. F. *J. Phys. Chem. A* **2009**, *113*, 7360.
- (53) Flynn, S. D.; Skvortsov, D.; Morrison, A. M.; Liang, T.; Choi, M. Y.; Vilesov, A. F. *J. Phys. Chem. Lett.* **2010**, *1*, 2233.
- (54) Morrison, A. M.; Flynn, S. D.; Liang, T.; Douberly, G. E. *J. Phys. Chem. A* **2010**, *114*, 8090.
- (55) Gutberlet, A.; Schwaab, G.; Birer, Ö.; Masia, M.; Kaczmarek, A.; Forbert, H.; Havenith, M.; Marx, D. *Science* **2009**, *324*, 1545.
- (56) Zwier, T. S. *Science* **2009**, *324*, 1522.
- (57) Goyal, S.; Schutt, D. L.; Scoles, G. *Phys. Rev. Lett.* **1992**, *69*, 933.
- (58) Scoles, G.; Lehmann, K. K. *Science* **2000**, *287*, 2429.
- (59) Toennies, J. P.; Vilesov, A. F. *Angew. Chem., Int. Ed.* **2004**, *43*, 2622.
- (60) Marx, D.; Hutter, J. *Ab Initio Molecular Dynamics: Basic Theory and Advanced Methods*; Cambridge University Press: Cambridge, 2009.
- (61) Reichardt, C. *Solvents and Solvent Effects in Organic Chemistry*; Wiley-VCH: Weinheim, 2003.
- (62) Becke, A. D. *Phys. Rev. A* **1988**, *38*, 3098.
- (63) Lee, C.; Yang, W.; Parr, R. G. *Phys. Rev. B* **1988**, *37*, 785.
- (64) Troullier, N.; Martins, J. L. *Phys. Rev. B* **1991**, *43*, 1993.
- (65) Hutter, J.; et al. CPMD, 2008; www.cpmid.org.
- (66) Laio, A.; Parrinello, M. *Proc. Natl. Acad. Sci. U.S.A.* **2002**, *99*, 12562.
- (67) Iannuzzi, M.; Laio, A.; Parrinello, M. *Phys. Rev. Lett.* **2003**, *90*, 238302.
- (68) Car, R.; Parrinello, M. *Phys. Rev. Lett.* **1985**, *55*, 2471.
- (69) Laio, A.; Parrinello, M. *Lect. Notes Phys.* **2006**, *703*, 315.
- (70) Ensing, B.; De Vivo, M.; Liu, Z.; Moore, P.; Klein, M. L. *Acc. Chem. Res.* **2006**, *39*, 73.
- (71) Scheidemann, A.; Schilling, B.; Toennies, J. P. *J. Phys. Chem.* **1993**, *97*, 2128.
- (72) Lewerenz, M.; Schilling, B.; Toennies, J. P. *J. Chem. Phys.* **1995**, *102*, 8191. Comment: Macler, M.; Bae, Y. K. *J. Chem. Phys.* **1997**, *106*, 5785. Reply: Lewerenz, M.; Schilling, B.; Toennies, J. P. *J. Chem. Phys.* **1997**, *106*, 5787.
- (73) Smith, I. W. M.; Sims, I. R.; Rowe, B. R. *Chem.-Eur. J.* **1997**, *3*, 1925.
- (74) Smith, I. W. M.; Rowe, B. R. *Acc. Chem. Res.* **2000**, *33*, 261.
- (75) Smith, I. W. M. *Chem. Rev.* **2003**, *103*, 4549.
- (76) Smith, I. W. M. *Angew. Chem., Int. Ed.* **2006**, *45*, 2842.
- (77) Smith, I. W. M., Ed. *Low Temperatures and Cold Molecules*; Imperial College Press: London, 2008.
- (78) Burnham, C. J.; Xantheas, S. S.; Miller, M. A.; Applegate, B. E.; Miller, R. E. *J. Chem. Phys.* **2002**, *117*, 1109.
- (79) Douberly, G. E.; Miller, R. E. *J. Phys. Chem. B* **2003**, *107*, 4500.
- (80) Mardyukov, A.; Sanchez-Garcia, E.; Rodziewicz, P.; Doltsinis, N. L.; Sander, W. *J. Phys. Chem. A* **2007**, *111*, 10552.
- (81) Rodziewicz, P.; Doltsinis, N. L. *J. Phys. Chem. A* **2009**, *113*, 6266.